IOPscience iopscience.iop.org

Home Search Collections Journals About Contact us My IOPscience

Gate-controlled mid-infrared light bending with aperiodic graphene nanoribbons array

This content has been downloaded from IOPscience. Please scroll down to see the full text.

2015 Nanotechnology 26 134002

(http://iopscience.iop.org/0957-4484/26/13/134002)

View the table of contents for this issue, or go to the journal homepage for more

Download details:

IP Address: 128.101.167.62
This content was downloaded on 06/10/2015 at 15:41

Please note that terms and conditions apply.

IOP Publishing Nanotechnology
Nanotechnology **26** (2015) 134002 (7pp) doi:10.1088/0957-4484/26/13/134002

Gate-controlled mid-infrared light bending with aperiodic graphene nanoribbons array

Eduardo Carrasco[1,5], Michele Tamagnone[1,2,5], Juan R Mosig[2], Tony Low[3,4] and Julien Perruisseau-Carrier[1]

[1] Adaptive MicroNano Wave Systems, Ecole Polytechnique Federale de Lausanne (EPFL), 1015 Lausanne, Switzerland
[2] Laboratory of Electromagnetics and Acoustics (LEMA), Ecole Polytechnique Federale de Lausanne (EPFL), 1015 Lausanne, Switzerland
[3] Department of Physics & Electrical Engineering, Columbia University, NY 10027, USA
[4] Department of Electrical & Computer Engineering, University of Minnesota, MN 55455, USA

E-mail: tlow@umn.edu

Received 15 December 2014, revised 21 January 2015
Accepted for publication 22 January 2015
Published 11 March 2015

Abstract

Graphene plasmonic nanostructures enable subwavelength confinement of electromagnetic energy from the mid-infrared down to the terahertz frequencies. By exploiting the spectrally varying light scattering phase at the vicinity of the resonant frequency of the plasmonic nanostructure, it is possible to control the angle of reflection of an incoming light beam. We demonstrate, through full-wave electromagnetic simulations based on Maxwell equations, the electrical control of the angle of reflection of a mid-infrared light beam by using an aperiodic array of graphene nanoribbons, whose widths are engineered to produce a spatially varying reflection phase profile that allows for the construction of a far-field collimated beam towards a predefined direction.

Keywords: graphene, plasmon, metamaterials

(Some figures may appear in colour only in the online journal)

Introduction

Graphene plasmonics has emerged as a very promising candidate for terahertz to mid-infrared applications [1], namely the frequency range where it supports plasmonic propagation. [1, 3–10]. Today the terahertz to mid-infrared spectrum, ranging from 10 to 4000 cm^{-1}, is finding a wide variety of applications in information and communication, homeland security, military, medical sciences, chemical and biological sensing and spectroscopy, among many others [11–13]. The bi-dimensional and semi-metallic nature of graphene allows for electrical tunability not possible with conventional metals by simply biasing electrostatically the graphene device. In addition, graphene is also an excellent conductor of electricity, with highest attained carrier mobility reaching 1 000 000 $cm^2 Vs^{-1}$ in suspended samples [14] and 100 000 $cm^2 Vs^{-1}$ for ultra-flat graphene on boron nitride [15]. These attributes, in addition to its stability and compatibility with standard silicon processing technologies, have also raised interest in a myriad of graphene-based passive and active photonic [2, 22, 23] and terahertz devices [3, 7, 17–21].

Electromagnetic surfaces able to dynamically control the reflection angle of an incident beam have been studied for decades in the microwave community [16, 24], with applications in satellite communications, terrestrial and deep-space radio links. Non-conventional reflecting surfaces for optical frequencies have also been proposed recently, using metal elements having certain fixed configurations and operating in the plasmonic regime [25, 26]. However, the high carrier concentration in metals prohibits dynamic control of the reflected beams via these surface elements. In this letter, we show how the reflection angle of a mid-infrared incident beam can be electrically controlled with an aperiodic array of graphene nanoribbons, by utilizing its intrinsic plasmonic resonance behavior. We demonstrate that the proposed effect is

[5] These authors contributed equally.

 © 2015 IOP Publishing Ltd Printed in the UK

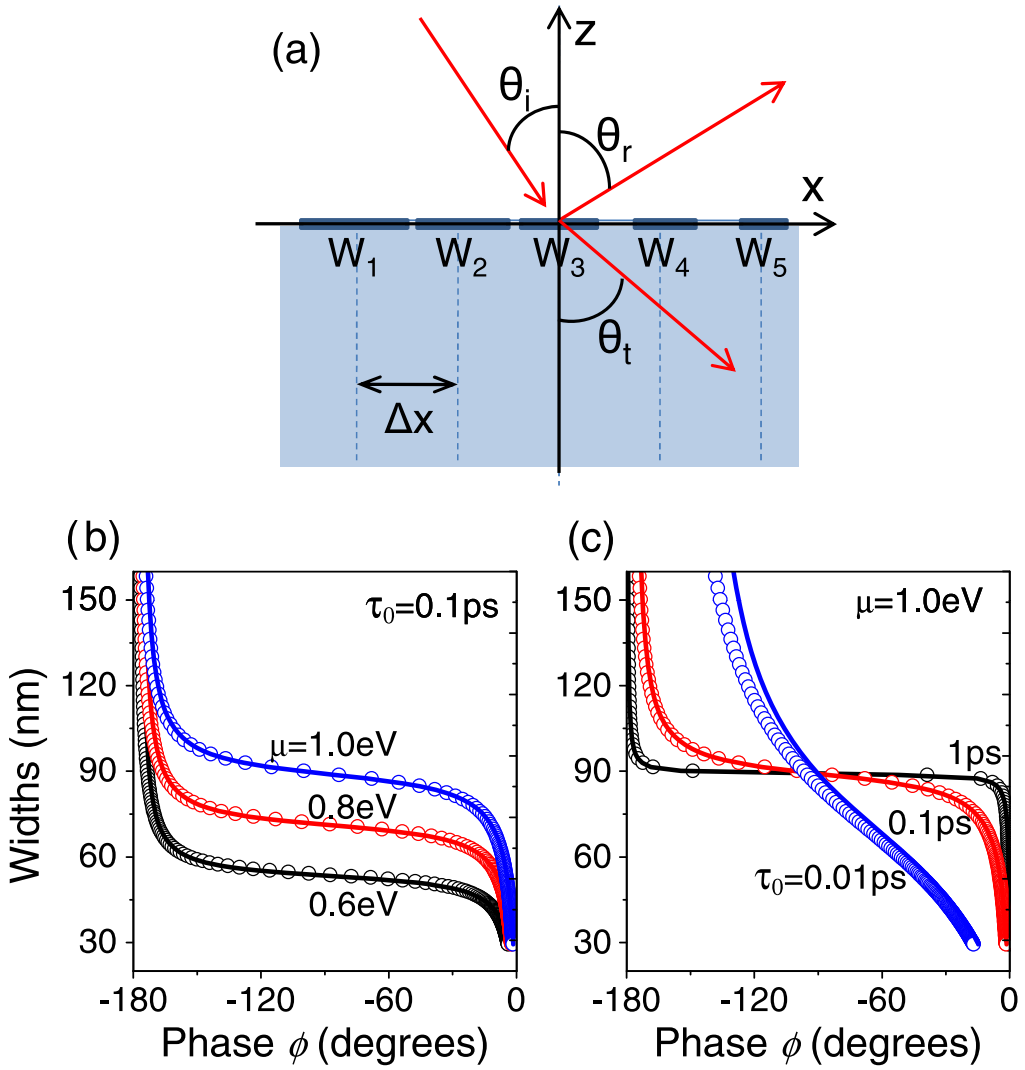

Figure 1. (a) Schematic illustrating the dynamic control of the angle of reflected and transmitted light by introducing gradient of scattering phases at the interface using graphene nanoribbon resonators with different widths. (b) And (c) calculated scattering phase ϕ for varying ribbons' width for p-polarized light with free-space wavelength $\lambda = 10\,\mu$m, e.g from a CO_2 laser. Calculations are done for different chemical potentials μ and electronic lifetimes τ_0 as shown. Symbols represent calculation from Maxwell equation, while solid lines are from simple model in equation (3).

experimentally realizable by performing numerical Maxwell simulations of the device with experimentally feasible parameters.

Basic concepts

Consider an aperiodic array of graphene nanoribbons of varying widths lying at the interface of two half spaces as illustrated in figure 1(a), with p-polarized light at incidence angle θ_i, which is reflected and transmitted at angle θ_r and θ_t respectively. Each nanoribbon constitutes a plasmonic resonator, which can effectively produce a scattering phase ϕ between 0 and $-\pi$ depending on the frequency of free-space light ω with respect to the plasmon resonance frequency ω_0. In plasmonic metasurfaces consisting of nanoribbons of varying widths, the scattering phase in general can also vary across the interface, namely as $\phi(x_j)$, where $x_j = j\Delta x$ and Δx being the distance between the centers of adjacent ribbons, which is considered constant in this contribution. In the limit where ray optics is applicable, i.e. $\lambda \gg \Delta x$, where λ is the free-space wavelength, the generalized Snell's law dictates that [25]

$$\sin(\theta_t)\sqrt{\epsilon_2} - \sin(\theta_i)\sqrt{\epsilon_1} = \frac{\lambda}{2\pi}\frac{d\phi}{dx},$$
$$\sin(\theta_r) - \sin(\theta_i) = \frac{\lambda}{2\pi\sqrt{\epsilon_1}}\frac{d\phi}{dx}. \quad (1)$$

Equation (1) implies that the reflected or transmitted beam can be effectively bent such that $\theta_r \neq \theta_{i,t}$ if a constant spatial gradient in the scattering phase is imposed (i.e. $d\phi/dx$ = constant). Simple estimates from equation (1) suggest that it is possible to bend normal incident ($\theta_i = 0$) mid-infrared light far from broadside (i.e. $\theta_r \neq 0$). Assuming $\lambda = 10\,\mu$m (e.g from a CO_2 laser), $\Delta x = 100$ nm (typical ribbon width where plasmon resonance resides in the mid-

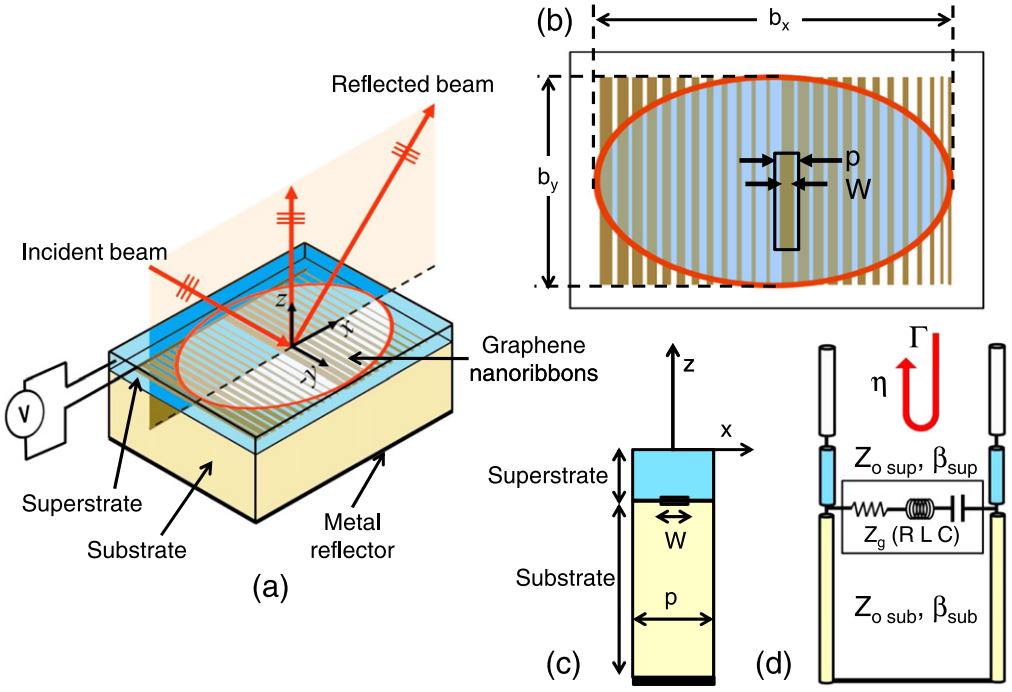

Figure 2. (a) Schematic of the gate-controlled reflectarray device based on aperiodic array of graphene nanoribbons. (b) Top view of the graphene nanoribbons array, including the elliptical projection of the impinging beam. (c) Lateral view of the device, highlighting the superstrate, substrate, ribbons, and metal reflector. (d) Equivalent circuit for one element of the proposed array.

infrared), one obtains $\Delta\phi \ll \pi$, suggesting that it is indeed possible to induce a gradual spatial variation in ϕ across the interface.

The scattering phase due to a graphene plasmonic resonator, and its design space, can be examined more quantitatively as follows. We consider graphene on a SiO_2 substrate and with an electrolyte superstrate, which can also serve as a top gate for inducing high doping in graphene [28]. We solve the Maxwell equations for the reflection coefficient of a *p*-polarized light, $r_p(q, \omega)$, where graphene is modeled by its dynamic local conductivity $\sigma(\omega)$ obtained from the random phase approximation [29, 30]. The scattering phase ϕ then follows from $\phi(q, \omega) = \arg[r_p(q, \omega)]$. The nanoribbon resonator frequency ω_0 can be estimated from the scattering coefficients for a continuous monolayer, where the in-plane wave–vector q is related to the width W of the nanoribbon via $q = 3\pi/4W$, after accounting for the anomalous reflection phase off the edges [27]:

$$\omega_0 = \sqrt{\frac{3e^2\mu}{8W\hbar^2\epsilon_{env}}}, \tag{2}$$

where $\epsilon_{env} = \frac{1}{2}(\epsilon_1 + \epsilon_2)$, ϵ_1 and ϵ_2 are the relative permittivities of the superstrate and substrate respectively. The Lorentz oscillator model provides then a simple expression for the scattering phase:

$$\phi(W, \omega) \approx \tan^{-1}\left(\frac{\omega}{\tau_0}\left(\omega^2 - \frac{3e^2\mu}{8W\hbar^2\epsilon_{env}}\right)^{-1}\right). \tag{3}$$

In this simple model calculation, we simply take $\epsilon_2 = 3.9$ and $\epsilon_1 = 6$. Assuming $\lambda = 10\,\mu$m, figures 1(b)–(c) depicts $\phi(W, \omega)$ for varying W, with graphene at different chemical potentials μ, and electronic lifetimes τ_0. The phase ϕ changes most rapidly with W when the ribbon is at resonance. For a given ribbon plasmon resonance frequency, increasing the doping would allow for the same resonance frequency at a larger W as depicted in figure 1(b). On the other hand, decreasing τ_0 dampens the plasmon resonance, causing a smoother variation in ϕ with W as shown in figure 1(c). This dampening can be understood, considering the quality factor of the plasmonic resonance, which is proportional to $\tau\omega$ i.e. a lower quality factor implies a smoother phase step. Equation (3) therefore provides a simple intuitive understanding of the scattering phase of a graphene plasmonic resonator.

Device simulation

In principle, the tunable scattering phase of a graphene plasmonic resonator allows the design of surface elements which controls the angle of reflection or transmission of an incoming beam. In this work, we consider the former i.e. a reflectarray [16]. Figures 2(a)–(b) shows a detailed schematic of the proposed device, designed for a working frequency of 27 THz (900 cm^{-1}). The graphene nanoribbons array is between an electrolyte gating superstrate of 200 nm and a 1.2 μm SiO_2 dielectric substrate with a metal layer underneath, which serves as a reflector, reflecting most of the incoming light. The full dielectric function of SiO_2 is used in the simulation [31]. For the electrolyte superstrate,

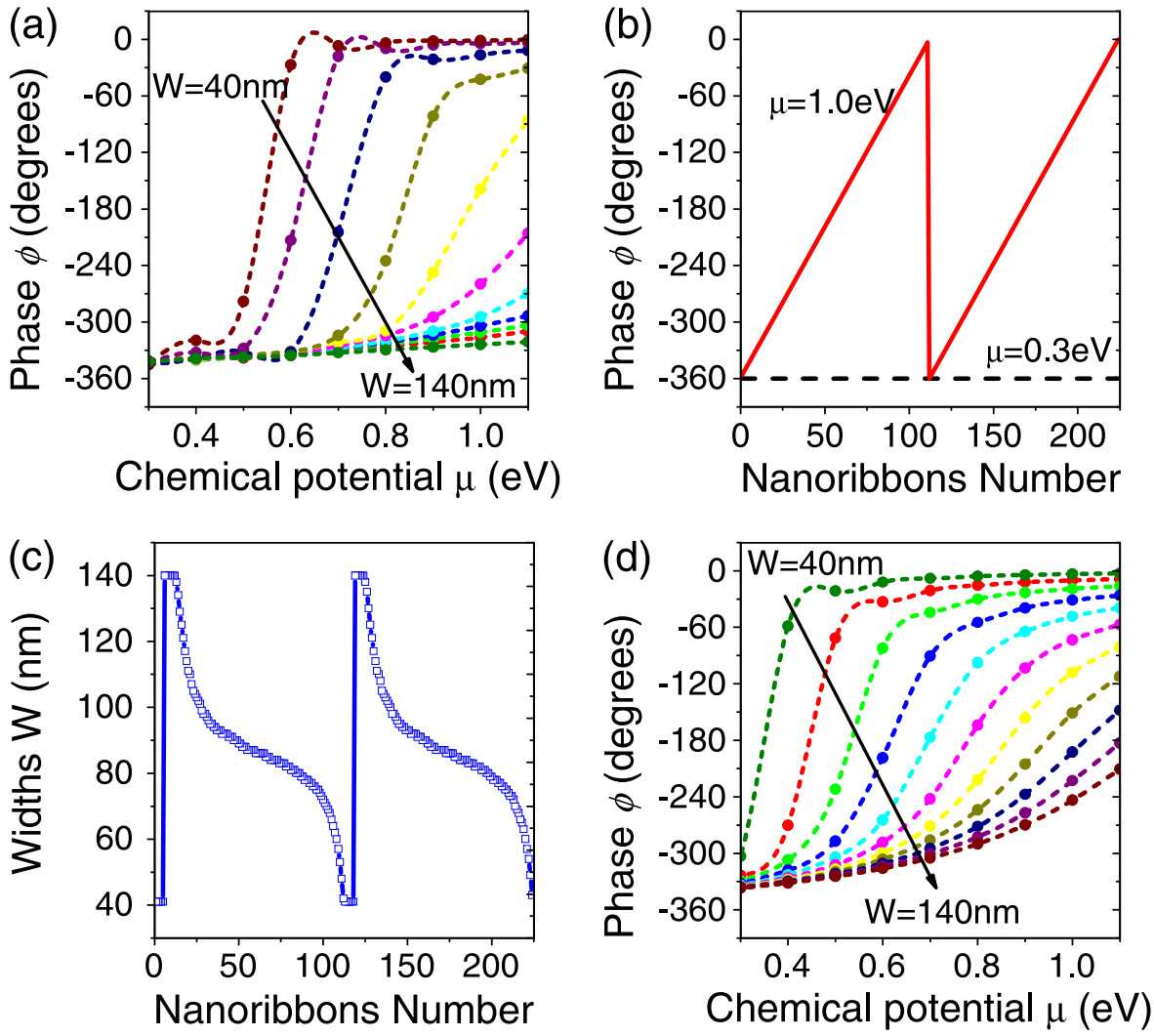

Figure 3. (a) Phase ϕ of the reflection coefficient as a function of chemical potential μ for different widths W of a nanoribbon, ranging from 40 to 140 nm. Mutual coupling between neighboring ribbons is taken into account. (b) Spatial phase profile required at each nanoribbon along the x-axis in order to produce a far-field beam in the broadside direction (0°) and a reflected far-field beam in the specular direction (45°). (c) Width of the nanoribbons across the array (x-axis) of the reflectarray device. (d) Phase ϕ of the reflection coefficient as a function of chemical potential μ for different widths W of a nanoribbon using the equivalent circuit model described in figure 2(d).

we assumed a dielectric constant of 6. Hence, the effective dielectric constant of the graphene's environment, which ultimately determines its plasmonic response, is approximately five, similar to [3]. The aperiodic array of nanoribbons has a designed inter-ribbon separation p taken to be 140 nm, and the width of each nanoribbons is to be chosen so that the spatial variation in ϕ_r satisfies $\mathrm{d}\phi_r/\mathrm{d}x = \text{constant}$, as discussed previously. As explained later, the final reflection phase ϕ_r of the reflecting cell is not given simply by the response ϕ of the ribbon, since the contribution of the ground plane must also be taken into account. We consider a Gaussian beam illuminating the array at an incident angle 45° with respect to the normal of the xz plane as illustrated. Figure 2(c) depicts the top view of the nanoribbons array, including the elliptical projection of the impinging beam on the xz plane, where $b_x = 31.36\,\mu$m and $b_y = 22.18\,\mu$m.

We use CST microwave studio to numerically compute the reflection coefficient and ϕ_r for a nanoribbon of particular width. Using the Floquets theory for periodic arrays, mutual coupling between neighboring nanoribbons is accounted for. Graphene is modeled (using a 2D boundary condition) by its local dynamic conductivity $\sigma(\omega)$, assuming typical electronic lifetime of $\tau_0 = 0.1$ ps. Figure 3(a) shows the calculated ϕ_r of the reflection coefficient, as a function of the chemical potential μ and width W of the nanoribbon. For a chemical potential $\mu = 1.0$ eV, ϕ_r varies between 0° and −340° by adjusting the width of the ribbons between 40 and 140 nm. As μ decreases, the range of ϕ_r decreases, which approaches a constant $\phi_r = -340°$ at $\mu = 0.3$ eV.

We design the reflectarray device to perform a binary operation: consisting of producing a reflected far-field beam in the broadside direction (0°) and a reflected far-field beam in the specular direction (45°). The spatial phase profile required

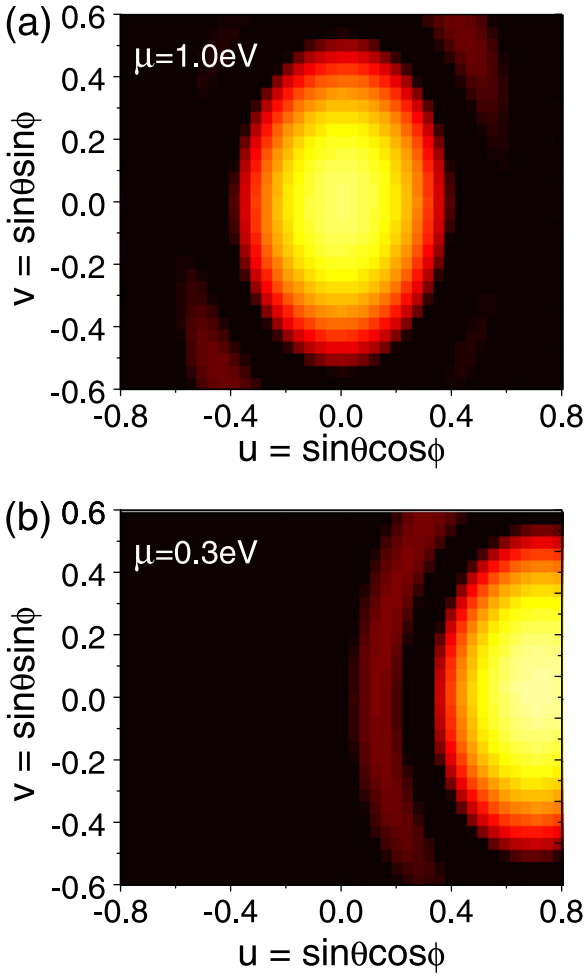

Figure 4. Far-field radiation pattern produced by the reflective array for the two bias condition; (a) beam towards broadside (0°) at μ = 1.0 eV and (b) specular direction (45°) at μ = 0.3 eV.

to achieve these reflection angles can be determined based on equation (1), and are shown in figure 3(b) for these two cases. For specular beam, a zero phase difference between the nanoribbons would suffice, regardless of the absolute value of that phase. Otherwise, the sequence of ribbons' widths has to be chosen such that it provides the neccessary spatial phase profile to produce a reflected far-field beam at μ = 1.0 eV. As mentioned above, with ribbons between 40 and 140 nm, ϕ_r can be made to vary between 0° and −340°. The missing phase values (from −340° to −360°) were found not to have noticeable impact in the far-field generation. The widths of the nanoribbons along the array are displayed in figure 3(c). In order to produce a reflected far-field beam in the specular direction, a constant ϕ_r is required along all the elements of the array. This can be achieved by decreasing μ to 0.3 eV as shown. In other words, the binary operation of our reflectarray device can be achieved by electrically controlling the doping μ.

In figures 4(a) and (b), we compute the far-field produced by our reflectarray device, for broadside (μ = 1.0 eV) and specular radiation (μ = 0.3 eV) respectively. The possibility of bending the light beam in an aperiodic array of graphene nanoribbons is clearly demonstrated by these simulations.

Discussion

A constant phase gradient is needed for producing a collimated beam. At intermediate dopings, where the ribbon array phases are not designed with constant phase gradient, the produced far field beam can be highly distorted. The design of smooth beam steering is possible, but would require a more complicated gating scheme that addresses the doping of individual ribbons separately as typically done in microwave reflectarrays [33] and more recently also for terahertz graphene-based reflectarrays [32]. The simplicity in the reflectarray array scheme proposed in this work has the obvious appeal of providing a design much easier to be implemented experimentally.

A simple circuit model for each nanoribbon cell, as shown in figure 2(d), is useful for better understanding of the proposed device. The substrate and superstrate can be modelled with two transmission line segments having propagation constants and characteristic impedance equal to the two media which they model. The equivalent of the ground plane is simply a short circuit, while the graphene ribbons can be represented by an equivalent Z_g impedance in parallel, that models the surface currents induced in the ribbons by the tangential electric field. An approximate closed form expression for Z_g can be found by modeling resonant ribbons as Lorentz oscillators as explained previously. This can be represented by a simple RLC series circuit, where R and L are simply found from the real and imaginary parts of the surface conductivity of graphene σ, while C represents the quasi-static electric fields associated with the plasmons, and can be obtained by enforcing the resonant frequency of the RLC circuit ($1/\sqrt{LC}$) to be equal to the ribbons resonant frequency ω_0:

$$L = \frac{\pi\hbar^2}{e^2\mu}, \quad R = \tau^{-1}L, \quad C = \frac{1}{\omega_0^2 L}, \tag{4}$$

where

$$\omega_0 \approx \sqrt{\frac{3e^2\mu}{8W\hbar^2\epsilon_{env}}}. \tag{5}$$

The final equivalent impedance of graphene nanoribbons is then

$$Z_g = R + j\omega L + \frac{1}{j\omega C} = \frac{\pi\hbar^2}{e^2\mu}\left(\frac{\omega_0^2 + j\omega\tau^{-1} - \omega^2}{j\omega}\right). \tag{6}$$

This circuit model provides for an estimated value for the reflection phase ϕ_r as function of W and μ. Figure 3(d) shows the calculated reflection phase ϕ_r which agrees qualitatively

with the numerical simulations presented in figure 3(a). The full wave simulations account for higher order phenomena not captured by this simple model. Importantly, while in the Lorentz oscillator the phase range is always less than π for the nanoribbons alone (i.e. equation (3)), the presence of the substrate and of the ground plane allows here a much wider phase range, which is a key point for the device presented in our work.

Our device has an average element loss of 1.32 dB for the $\mu = 0.3$ eV configuration, and 1.77 dB for $\mu = 1$ eV. Hence, most of the incoming light is reflected. The loss of the device is directly related to the assumed electronic lifetime τ, as evident from equation (4), and can be improved with better graphene quality or by using a better substrate such as boron nitride [34].

Conclusion

In this work, we show how the reflection angle of a mid-infrared beam can be dynamically controlled by employing tunable graphene plasmons in an aperiodic array of graphene nanoribbons according to the generalized laws of reflection. The use of a simple gating scheme makes the proposed design particularly attractive because of its easy experimental fabrication. Numerical Maxwell device simulations convincingly demonstrate the dynamic bending of mid-infrared beams, assuming experimentally accessible physical parameters.

Acknowledgments

This work was supported by the European Union (Marie Curie IEF 300934 RASTREO project), the Hasler Foundation (Project 11149) and the Swiss National Science Foundation (Project 133583), and the University of Minnesota. E Carrasco, M Tamagnone, T Low and JR Mosig would like to dedicate this paper to the memory of J Perruisseau-Carrier, who passed away during the preparation of this work.

References

[1] Low T and Avouris P 2014 Graphene plasmonics for terahertz to mid-infrared applications *ACS Nano* **8** 1086–101
[2] Tamagnone M, Fallahi A, Mosig J R and Perruisseau-Carrier J 2014 Fundamental limits and near-optimal design of graphene modulators and non-reciprocal devices *Nat. Photonics* **8** 556–63
[3] Ju L *et al* 2011 Graphene plasmonics for tunable terahertz metamaterials *Nat. Nanotechnology* **6** 630–4
[4] Koppens F H, Chang D E and Garcia de Abajo F J 2011 Graphene plasmonics: a platform for strong lightmatter interactions *Nano Lett.* **11** 3370–7
[5] Grigorenko A N, Polini M and Novoselov K S 2012 Graphene plasmonics *Nat. Photonics* **6** 749–58
[6] Yan H, Low T, Zhu W, Wu Y, Freitag M, Li X, Guinea F, Avouris P and Xia F 2013 Damping pathways of mid-infrared plasmons in graphene nanostructures *Nat. Photonics* **7** 394–9
[7] Yan H, Li X, Chandra B, Tulevski G, Wu Y, Freitag M, Zhu W, Avouris P and Xia F 2012 Tunable infrared plasmonic devices using graphene/insulator stacks *Nat. Nanotechnology* **7** 330–4
[8] Chen J *et al* 2012 Optical nano-imaging of gate-tunable graphene plasmons *Nature* **487** 77–81
[9] Fei Z *et al* 2012 Gate-tuning of graphene plasmons revealed by infrared nano-imaging *Nature* **487** 82–5
[10] Jablan M, Buljan H and Soljai M 2009 Plasmonics in graphene at infrared frequencies *Phys. Rev.* B **80** 245435
[11] Tonouchi M 2007 Cutting-edge terahertz technology *Nat. Photonics* **1** 97–105
[12] Ferguson B and Zhang X-C 2002 Materials for terahertz science and technology *Nat. Mater.* **1** 26–33
[13] Soref R 2010 Mid-infrared photonics in silicon and germanium *Nat. Photonics* **4** 495–7
[14] Du X, Skachko I, Barker A and Andrei E Y 2008 Approaching ballistic transport in suspended graphene *Nat. Nanotechnology* **3** 491–5
[15] Dean C R *et al* 2010 Boron nitride substrates for high-quality graphene electronics *Nat. Nanotechnology* **5** 722–6
[16] Huang J and Encinar J A 2008 *Reflect array Antennas* (USA: IEEE Press)
[17] Chen P Y and Alu A 2013 Terahertz metamaterial devices based on graphene nanostructures *IEEE Trans. Terahertz Sci. Tech.* **3** 748–56
[18] Padooru Y R, Yakolev A B, Kaipa C S R, Hanson G W, Medina F and Mesa F 2013 Dual capacitive–inductive nature of periodic graphene patches: transmission characteristics at low terahertz frequencies *Phys. Rev.* B **87** 115401
[19] Lee S H *et al* 2012 Switching terahertz waves with gate-controlled active graphene metamaterials *Nat. Mater.* **11** 936–41
[20] Otsuji T, Tombet S B, Satou A, Fukidome H, Suemitsu M, Sano E, Popov V, Ryzhii M and Ryzhii V 2012 Graphene-based devices in terahertz science and technology *J. Phys. D: Appl. Phys.* **45** 303001
[21] Vicarelli L, Vitiello M S, Coquillat D, Lombardo A, Ferrari A C, Knap W, Polini M, Pellegrini V and Tredicucci A 2012 Graphene field-effect transistors as room-temperature terahertz detectors *Nat. Mater.* **11** 865–71
[22] Bao Q and Loh K P 2012 Graphene photonics, plasmonics, and broadband optoelectronic devices *ACS Nano* **6** 3677–94
[23] Bonaccorso F, Sun Z, Hasan T and Ferrari A C 2010 Graphene photonics and optoelectronics *Nat. Photonics* **4** 611–22
[24] Hum S and Perruisseau-Carrier J 2013 Reconfigurable reflectarrays and array lenses for dynamic antenna beam control: a review *IEEE Trans. on Antennas and Propagation* **62** 183–198
[25] Yu N, Genevet P, Kats M A, Aieta F, Tetienne J-P, Capasso F and Gaburro Z 2011 Light propagation with phase discontinuities: generalized laws of reflection and refraction *Science* **334** 333–7
[26] Ni X, Emani N K, Kildishev A V, Boltasseva A and Shalaev V M 2012 Broadband light bending with plasmonic nanoantennas *Science* **335** 427–427
[27] Nikitin A Y, Low T and Martin-Moreno L 2014 Anomalous reflection phase of graphene plasmons and its influence on resonators *Phys. Rev.* B **90** 041407
[28] Efetov D K and Kim P 2010 Controlling electron–phonon interactions in graphene at ultrahigh carrier densities *Phys. Rev. Lett.* **105** 256805
[29] Wunsch B, Stauber T, Sols F and Guinea F 2006 Dynamical polarization of graphene at finite doping *New J. Phys.* **8** 318

[30] Hwang E H and Sarma S D 2007 Dielectric function, screening, and plasmons in two-dimensional graphene *Phys. Rev.* B **75** 205418
[31] Palik E D (ed) 1998 *Handbook of Optical Constants of Solids* vol 3 (New York: Academic)
[32] Carrasco E, Tamagnone M and Perruisseau-Carrier J 2013 Tunable graphene reflective cells for THz reflectarrays and generalized law of reflection *Appl. Phys. Lett.* **102** 104103
[33] Kamoda H, Iwasaki T, Tsumochi J, Kuki T and Hashimoto O 2011 60 GHz electronically reconfigurable large reflectarray using single-bit Phase shifters *IEEE Trans. Antennas Propag.* **59** 2524–31
[34] Woessner A *et al* 2014 Highly confined low-loss plasmons in graphene–boron–nitride heterostructures *Nat. Materials* at press (doi:10.1038/nmat4169)